*Inflammatory Bowel Diseases*, 2023, **29**, 1133–1144
https://doi.org/10.1093/ibd/izad003
Advance access publication 23 January 2023
**Original Research Articles - Basic Science**

# Inhibition of Soluble Stem Cell Factor Promotes Intestinal Mucosal Repair

**Vicky Garcia-Hernandez, PhD, Arturo Raya-Sandino, PhD, Veronica Azcutia, PhD, Jael Miranda, PhD, Matthias Kelm, MD, Sven Flemming, MD, Dorothee Birkl, MD, Miguel Quiros, PhD, Jennifer C. Brazil, PhD, Charles A. Parkos, MD, PhD, and Asma Nusrat, MD**

Department of Pathology, University of Michigan Medical School, Ann Arbor, MI, USA

**Address correspondence to:** Asma Nusrat, MD, University of Michigan Medical School, Department of Pathology, 4057 BSRB, 109 Zina Pitcher Place, Ann Arbor, MI 48109, USA. Phone: (734) 764-5712, (anusrat@umich.edu).

**Background:** Incidences of inflammatory bowel disease (IBD), including Crohn's disease and ulcerative colitis, are escalating worldwide and can be considered a global public health problem. Given that the gold standard approach to IBD therapeutics focuses on reducing the severity of symptoms, there is an urgent unmet need to develop alternative therapies that halt not only inflammatory processes but also promote mucosal repair. Previous studies have identified increased stem cell factor (SCF) expression in inflamed intestinal mucosal tissues. However, the role that SCF plays in mediating intestinal inflammation and repair has not been explored.

**Methods:** Changes in the expression of SCF were evaluated in the colonic tissue of healthy mice and during dextran sodium sulfate (DSS)-induced colitis. Furthermore, mucosal wound healing and colitis severity were analyzed in mice subjected to either mechanical biopsy or DSS treatment, respectively, following intestinal epithelial cell–specific deletion of SCF or anti-SCF antibody administration.

**Results:** We report robust expression of SCF by intestinal epithelial cells during intestinal homeostasis with a switch to immune cell-produced SCF during colitis. Data from mice with intestinal epithelial cell–specific deletion of SCF highlight the importance of immune cell–produced SCF in driving the pathogenesis of colitis. Importantly, antibody-mediated neutralization of total SCF or the specific $SCF^{248}$ isoform decreased immune cell infiltration and enhanced mucosal wound repair following biopsy-induced colonic injury or DSS-induced colitis.

**Conclusions:** These data demonstrate that SCF functions as a pro-inflammatory mediator in mucosal tissues and that specific neutralization of $SCF^{248}$ could be a viable therapeutic option to reduce intestinal inflammation and promote mucosal wound repair in individuals with IBD.

## Lay Summary

Our investigation demonstrates that blocking cleavable $SCF^{248}$ isoform by administration of specific stem cell factor antibodies enhances healing of the intestinal mucosa and restores critical barrier function, suggesting an alternative therapeutic option to treat individuals with active IBD.

**Key words:** epithelia, pro-inflammatory cytokine, mucosal repair, IBD, intestine

## Introduction

Inflammatory bowel disease (IBD), including Crohn's disease (CD) and ulcerative colitis (UC), comprises a chronic and relapsing inflammatory disorder of the gastrointestinal tract.[1,2] Due to globally increasing incidence rates, IBD represents a serious worldwide health care burden.[3–5] Although the exact etiology of IBD remains largely unknown, its pathobiology is thought to involve complex interactions between genetic, environmental, or microbial factors combined with immune dysregulation.[6,7] The efficacy of current treatment strategies for IBD such as targeting tumor necrosis factor (TNF)-α or integrins to reduce mucosal inflammation is limited due to high rates of primary nonresponse, loss of response over time, and adverse off-target effects.[8] Therefore, there is an unmet need for novel therapeutic approaches that drive mucosal repair resulting in a full return to a healthy intestinal mucosa.

Stem cell factor (also known as SCF, KIT-ligand, or steel factor) is a pleiotropic cytokine that mediates regulatory effects on inflammation, tissue remodeling, and fibrosis through binding to its receptor c-KIT.[9–12] Stem cell factor plays a well-described role in regulating the survival, proliferation, migration, and differentiation of hematopoietic progenitors, melanocytes, and germ cells. More recent studies have demonstrated SCF expression in dermal and intestinal epithelial cells.[13–15] Although increased SCF expression has been reported in the inflamed mucosa of individuals with IBD and colitic mice, the role of SCF during mucosal inflammation in the gut remains poorly understood.[15–18]

Previous studies have demonstrated that total inhibition of binding interactions between SCF and c-KIT results in undesirable off-target effects,[19–21] highlighting the need for more specific and refined approaches when it comes to SCF targeting. Endogenous SCF occurs in 2 main forms, a 248 amino acid (AA) cleavable form ($SCF^{248}$) and a 220 AA "noncleavable" form ($SCF^{220}$). In the present study, we investigated the role of $SCF^{248}$ and $SCF^{220}$ isoforms in regulating colonic inflammation and repair. Our data demonstrate increased expression of $SCF^{248}$ during colitis and

Received for publication: November 16, 2022. Editorial Decision: January 1, 2023

**Key messages**

**What is already known?**

The inhibition of the pro-inflammatory cytokine SCF promotes recovery after lung inflammation/fibrosis.

**What is new here?**

The immune cell–produced $SCF^{248}$ variant expression is increased during intestinal inflammation, and its inhibition promotes recovery after mucosal injury.

**How can this study help patient care?**

Targeted inhibition of $SCF^{248}$ may serve to improve clinical care and reduce rates of adverse events in IBD patients.

that targeted $SCF^{248}$ neutralization protects against dextran sodium sulfate (DSS)-induced damage by promoting intestinal mucosal wound healing. Studies using mice lacking expression of SCF in intestinal epithelial cells revealed that immune cell–produced rather than intestinal epithelial cell (IEC)-produced SCF drives pathogenesis during colitis. We also show that neutralization of SCF in vivo reduces leukocyte infiltration in response to DSS-induced colitis, suggesting that improved mucosal repair downstream of SCF inhibition is in part mediated by attenuating the lamina propria influx of immune cells. Collectively our results suggest that specific blockade of soluble SCF during intestinal inflammation might represent a novel therapeutic approach for promoting mucosal wound repair in individuals with IBD.

## Material and Methods

### Animals

Mice were kept under strict specific pathogen-free conditions with ad libitum access to normal chow and water. Wild type male C57BL/6 mice between 10 and 14 weeks were purchased from the Jackson Laboratory (C57BL/6J) and maintained at the University of Michigan (Ann Arbor, MI) under a 12-hour light/dark cycle. Mice with selective SCF deficiency in intestinal epithelial cells (IECs) were generated on a C57BL/6 background by breeding SCF floxed mice ($Kitlg^{f/f}$) with mice expressing the inducible mutated estrogen receptor fused to Cre-recombinase under control of the Villin promoter: *Villin*-$Cre^{ERT2}$; $Kitlg^{f/f}$ ($Kitlg^{ER\Delta IEC}$). Mice were bred *in house* at the University of Michigan and maintained as described previously. Eight-week-old $Kitlg^{ER\Delta IEC}$ and control littermates $Kitlg^{f/f}$ mice were injected intraperitoneally (i.p.) with 1 mg/100 µL of tamoxifen (Sigma, T5648) dissolved in sterile corn oil (Sigma, C8267) for 5 consecutive days. Animals were used 4 weeks after the final tamoxifen injection. All experiments were approved and conducted in accordance with guidelines set by the University of Michigan Institutional Animal Care and Use Committee.

### DSS-induced Experimental Colitis

Mice were provided with 3% (w/v) 40-50 kDa DSS (Alfa Aesar, Affymetrix, Cat. 9011-18-1,) dissolved in drinking water ad libitum for 5 days followed by a recovery period of 3 or 5 days with normal drinking water (DSS colitis/recovery model) or with 3 cycles of 3% DSS dissolved in drinking water ad libitum for 5 days followed by a recovery period of 4 days with drinking water (chronic DSS colitis).

### Disease Activity Index and Histological Colitis Score

Clinical disease assessment was performed daily, with scores of 0 to 4 assigned for body weight loss, stool consistency, and presence of blood in stools (Fisher HealthCare, Fecal Occult Blood Test-E.S, Cat. 23038035). Individual scores were added, and averages were recorded as disease activity index (DAI), with higher values reflecting the increasing severity of colitis. At the end of the experiment, mice were humanely euthanized, and colonic tissue was formalin-fixed and paraffin-embedded (FFPE). Hematoxylin-eosin (H&E) staining of sections of Swiss roll mounts of the entire colon (4-µm thick) was performed to quantify colonic mucosal injury by calculation of histological colitis score (HCS), a metric which considers the length of injured/ulcerated area (≥50% crypt loss) relative to the length of the entire colon.[22] Slides were scanned using an Aperio AT2 from Leica Biosystems, with a resolution of 0.25 µm per pixel using a 40x objective. The total length, areas of inflammation, and ulceration were measured by 2 independent investigators using Aperio ImageScope 12 (Leica Biosystems).

### Wound Healing Assay

In vivo wound healing assays were performed using a high-resolution video endoscope (Coloview Veterinary Endoscope, Karl Storz) equipped with biopsy forceps (Karl Storz; Germany) as described previously.[23,24] Briefly, biopsy-induced mucosal wounds were generated at 3 to 5 sites along the dorsal aspect of the colon of anesthetized mice (i.p. injection of ketamine 100 mg/kg, xylazine 5 mg/kg). Wound healing was quantified at 1 and 3 days after injury. Endoscopic procedures were viewed with high-resolution (1024 × 768 pixels) images on a flat-panel color monitor. Each wound region was photographed at 1 and 3 days postinjury, and wound areas were calculated using ImageJ. In each experiment, 3 to 5 wounds per mouse were quantified.[25]

### Enzymatic Isolation of Subepithelial Lamina Propria-enriched cellular Fractions

Lamina propria (LP)-enriched fractions were isolated by enzymatical digestion at 37°C under mechanical agitation at 200 rpm (relative centrifugal force, RCF = 0.41 x g) in an Infors HT Ecotron orbital shaker (Infors AG, Bottmingen, Switzerland) as described previously.[23] Briefly, the distal colon was collected and opened longitudinally before mesenteric vessels were removed. Mucus layers were next removed by incubating the tissue in phosphate buffered saline (PBS) without calcium and magnesium (PBS–) supplemented with 2% fetal bovine serum (FBS) and 5 mM of dithiothreitol (DTT) (Fisher BioReagents, BP1725) for 20 minutes. Intestinal epithelial cells were then removed by 3 consecutive washes in chelating buffer (PBS– containing 2% FBS and 5 mM etheylenediamine tetraacetic acid (EDTA). Lonza, Cat. 51201). The remaining tissue was minced into small (<1 $mm^2$) pieces and digested in Hanks' balanced salt solution (HBSS) with calcium and magnesium (HBSS+) supplemented with 10 mM of HEPES (Corning, Cat. 25-060-CI), Liberase (37.5

U/mL; Roche Life Science Products, Cat. 5401127001,) and DNase I (300 Kuntz units/mL; EMD Millipore Corp., Cat. 260913,) for 30 minutes. Digested tissue was further disaggregated mechanically by passing the suspension through an 18-gauge needle, followed by filtration through a 70-µm cell strainer before washing in a solution of cold PBS– supplemented with 10% FBS and 2 mM of EDTA. Purity of LP-enriched fractions was determined by flow cytometry analysis.

## Flow Cytometry Analysis

Detailed information on antibodies is provided in Table 1; 2 x$10^6$ cells from LP-enriched fractions were stained under standard conditions. For dead cell exclusion, cells were stained with an eFluor780 live/dead discrimination dye (1:1000, eBiosciences, Cat. 65-0865). The Fc receptors were blocked using mouse Fc-block (CD16/CD32; dilution 1:100) followed by cell staining with the indicated cocktail of antibodies. Lineage markers were gated out using a PE dump channel (CD3, CD4, CD8, gdTCR, CD19, TER119; dilution 1:200), PercP-CD45+ (1:200), PE-Cy7-FceRI (1:400), Alexa Fluor 647-Ly6G (1:200), and BV421-SiglecF (1:200). After thorough washing with staining buffer, CountBright counting beads were added to determine the absolute number of cells according to the manufacturers' instructions (Invitrogen, Cat. C36950). Acquisition of stained cells was performed on a NovoCyte Flow Cytometer (ACEA Biosciences Inc. San Diego, CA). Data were analyzed using FlowJo v10.8.1 software (Tree Star, Ashland, OR).

## Neutralizing Antibodies

The anti-$SCF^{248\&220}$ polyclonal and anti-$SCF^{248}$ monoclonal antibodies were generated as previously described.[26,27] Polyclonal IgG (Lampire, Cat. 74060404) and mouse IgG1 kappa (K) isotype (Rockland, Cat. 010-001-330) were purified using protein A affinity chromatography. For DSS colitis, studies mice were intraperitoneally injected with either 3 mg/mouse of rabbit anti-$SCF^{248\&220}$ neutralizing antibody or control rabbit IgG antibody or with monoclonal anti-$SCF^{248}$ antibody or control IgG antibody at a concentration of 0.4 mg/mouse. For wounding experiments, 10 µg of anti-$SCF^{248\&220}$ or IgG control antibodies were injected into the wound bed as previously described.[28]

## Immunofluorescence Labelling

Tissues were formalin-fixed and embedded in paraffin (FFPE). Sections were cut at 4 µm, baked at 60°C for 1 hour, followed by deparaffinization, dehydration, and antigen retrieval for 15 minutes (Vector labs, Cat. H-3300). Sections were permeabilized/blocked with a solution of PBS+ containing 0.3% triton X-100 and 3% bovine serum albumin (BSA) for 1 hour at room temperature. The primary antibody was incubated in blocking solution (Thermo Fisher, SCF polyclonal antibody, 1:200, Cat. PA5-20746 and Cell Signaling, c-kit polyclonal antibody, 1:200, Cat. 3074) overnight at 4°C and washed with Hanks' balanced salt solution the following day. Secondary antibody incubations were performed for 1 hour, and nuclei were stained with DAPI (Thermo Fisher Scientific, 1:1000, Cat. D1306). Finally, samples were mounted using ProLong Gold antifade reagent (Thermo Fisher, Cat. P36930) and visualized using a Leica SP5 inverted microscope.

## RNAscope

The localization of *kitlg* and *kit* mRNA was performed by RNAscope in 8-µm sections of FFPE as previously reported.[29] Briefly, FFPE-colonic tissue sections were baked for 1 hour at 60°C, followed by deparaffinization, dehydration, and antigen retrieval at 100°C for 15 minutes (ACD, Cat. 322000). Tissues were digested by protease plus (ACD, Cat. 322331) for 15 minutes at 40°C. The RNAscope probes (ACD, Probe-Mm-Kitl, Cat. 423401, and Probe-Mm-kit, Cat.314151) were hybridized for 2 hours at 40°C, followed by signal amplification. Detection was performed according to RNAscope Multiplex Fluorescent Reagent Kit v2 (ACD, Cat. 323100). Nuclei were stained with DAPI (Thermo Fisher Scientific, 1:1000, Cat. D1306) for 10 minutes. Finally, samples were mounted using ProLong Gold antifade reagent (Thermo Fisher, Cat. P36930) and visualized using a Leica SP5 inverted microscope.

## Real-time Quantitative Polymerase Chain Reaction

Total RNA was isolated from the distal colon of mice using the RNeasy kit (Qiagen, Cat. 74106). The mRNA was purified using 20 µg of total RNA and the Dynabeads kit (Ambion, Cat. 61006); mRNA was reverse transcribed into cDNA using iScript Reverse Transcription Supermix (Bio-Rad, Cat. 1708841). Gene expression was evaluated by quantitative

**Table 1.** Antibodies used for flow cytometric characterization of the myeloid population in lamina propria of mouse colon.

| Lineage marker | Fluorochrome | Dilution | Cat. No. | Manufacturer |
|---|---|---|---|---|
| CD16/CD32 (Fc Blocker) | NA | 1:100 | 553142 | BD Pharmingen |
| CD3 | PE | 1:200 | 553063 (Clone 145-2C11) | BD Pharmingen |
| CD4 | PE | 1:200 | 553049 (Clone RM4-5) | BD Pharmingen |
| CD8 | PE | 1:200 | 100708 (Clone 53-6.7) | BioLegend |
| γδTCR | PE | 1:200 | 12-5711-82 (Clone eBioGL3) | Invitrogen |
| CD19 | PE | 1:200 | 12-0193-83 (Clone eBio1D3) | Invitrogen |
| TER119 | PE | 1:200 | 116208 (Clone TER-119) | BioLegend |
| CD45+ | PercP | 1:200 | 557235 (Clone 30-F11) | BD Pharmingen |
| FceRI* | PE-Cy7 | 1:400 | 134318 (Clone: MAR-1) | BioLegend |
| Ly6G | Alexa Fluor 647 | 1:200 | 108418 (Clone: RB6-8C5) | BioLegend |
| SiglecF | BV421 | 1:200 | 562681 (Clone E50-2440) | BD Biosciences |

PCR (qPCR) using SsoAdvanced Universal SYBR (Bio-Rad, Cat. 172574) with a Bio-Rad CTX Cycler measuring SYBR green incorporation. Reactions were performed in triplicate with at least 3 biological replicates. Relative expression of genes of interest was calculated using the $2^{-\Delta\Delta Ct}$ method with normalization to the housekeeping gene ribosomal protein 18 (Rp18). Primer sequences were as follows: *Kitlg*$^{248}$ (forward) 5'-GCCAGAAACTAGATCCTTTACTGA-3'; *Kitlg*$^{248}$ (reverse) 5'-ACATAAATGGTTTTGTGACACTGACTCTG-3'; *Kitlg*$^{220}$ (forward) 5'-CCCGAGAAAGGGAAAGCCG-3'; *Kitlg*$^{220}$ (reverse) 5'-ATTCTCTCTTTCTGTTGCAACATACTT-3'; *Kitlg*$^{248\&220}$ (forward) 5'-TTGTTACCTTCGCACAGTGG-3'; *Kitlg*$^{248\&220}$ (reverse) 5'-AATTCAGTGCAGGGTTCACA-3'; *Rp18* (forward) 5'-ACTTTTGGGGCCTTCGTGTC-3'; *Rp18* (reverse) 5' GCCCAGAGACTCATTTCTTCTTG -3'; *Tnfa* (forward) 5'-CCACCACGCTCTTCTGTCTAC -3'; *Tnfa* (reverse) 5'-TGGGCTACAGGCTTGTCACT-3'; *Infg* (forward) 5'- AAGTGGCATAGATGTGGAAG -3'; *Infg* (reverse) 5'-GAATGCATCCTTTTTCGCCT-3'; *Il17a* (forward) 5'-TGCTACTGTTGATGTTGGGAC-3'; *Il17a* (reverse) 5'- AATGCCCTGGTTTTGGTTGAA -3'; *Il22* (forward) 5'-CAGAAGGTCCGATTTCAGTCCAG-3'; *Il22* (reverse) 5'-TCCCATTGGCTCTGTCCATACATC-3'; *Il23* (forward) 5' - ACTCAAGGACAACAGCCAGTTC-3'; *Il23* (reverse) 5' -TCCTAGTAGGGAGGTGTGAAGTTG-3'; *S100a9* (forward) 5'-CAAATGGTGGAAGCACAGTTGGCA-3'; *S100a9* (reverse) 5'-TTGTGTCCAGGTCCTCCATGATGT-3'.

## Results

### Expression of SCF and Its Receptor c-KIT in Intestinal Mucosa

To investigate SCF function, we first examined spatial expression of *Kitlg* (SCF) and its receptor *Kit* (c-KIT) in the intestinal mucosa. The RNAscope in situ hybridization of colonic tissue obtained from wild-type C57BL/6J mice revealed robust expression of *Kitlg* and *Kit* in intestinal epithelial cells (Figure 1A, arrow) with lower levels of expression detected in underlying lamina propria cells (***$P$ < .001, ***$P$ < .0001, Figure 1A, arrowhead). To complement spatial mRNA detection, immunofluorescence labeling for SCF and c-KIT protein was performed. Confocal microscopy analyses revealed expression of SCF protein in colonic epithelial cells residing in the lower third of intestinal crypts, whereas c-KIT protein expression was restricted to epithelial cells in the crypt-base (Figure 1B, arrow). In contrast, minimal SCF and c-KIT protein were identified in lamina propria cells (*$P$ < .05, ****$P$ < .0001, Figure 1B, arrowhead). These data indicate that under conditions of mucosal homeostasis, SCF and c-KIT are predominantly expressed in colonic intestinal epithelial cells (IECs).

### Intestinal Inflammation Induces Increased Mucosal Expression of SCF

Increased expression of SCF has been reported in the colonic mucosa of individuals with IBD[15,16,30] and asthma.[31] Two transmembrane isoforms SCF$^{220}$ and SCF$^{248}$ have been reported in humans and mice.[32] Although cleavage of SCF$^{248}$ generates a soluble product of 165 AA, previous work has reported that SCF$^{220}$ remains intact at the membrane. Therefore, we next analyzed changes in expression of specific SCF isoforms during intestinal inflammation and repair using a well-established dextran sodium sulfate (DSS) colitis and recovery model that involves 5 days of DSS administration followed by 5 days of recovery with drinking water.[22] Colitis severity was assessed by calculating the disease activity index (DAI), a composite score incorporating weight loss, stool consistency, and the presence of blood. As expected, DSS-treated mice had significantly increased DAI scores from day 1 to day 10 compared with control mice that were not exposed to DSS (****$P$ < .0001, Figure 1C). Evaluation of transcriptional levels of *Kitlg*$^{220}$ (SCF$^{220}$) and *Kitlg*$^{248}$ (SCF$^{248}$) isoforms in the colonic mucosa by RT-qPCR revealed significantly increased expression of *Kitlg*$^{248}$ mRNA (cleavable SCF) on day 5 of DSS treatment, with a peak in expression observed 2 days after mice were switched to water (day 7) and recovery to basal levels of expression observed by day 10. In contrast, decreased levels of *Kitlg*$^{220}$ mRNA were detected on day 5 (*$P$ < .05, ***$P$ < .001, Figure 1D). Taken together, data reveal robust upregulation of cleavable SCF$^{248}$ during intestinal inflammation, suggesting that this SCF variant may play an important role in the pathobiology of colitis.

Intestinal inflammation is characterized by mucosal infiltration of SCF-expressing leukocytes including eosinophils, neutrophils, and mast cells.[33,34] Therefore, we analyzed infiltrating leukocyte populations in the lamina propria during DSS-induced colitis and repair. Data revealed robust recruitment of neutrophils, mast cells, and eosinophils 2 days after mice had been switched from DSS to water (Neutrophils: ***$P$ = .0003, Mast cells: **$P$ = .0081, Eosinophils: **$P$ = .0041, Figure 1E). Given that this time point is when maximum expression of SCF$^{248}$ was detected, these data highlight the importance of SCF$^{248}$ for immune cell infiltration during colonic repair. We next sought to determine levels of SCF and c-KIT expression in lamina propria immune cells recruited during recovery from DSS-induced colitis. Immunofluorescence analyses revealed robust expression of both SCF and c-KIT proteins in lamina propria immune cells from inflamed colonic mucosa (***$P$ < .001, ****$P$ < .0001, Figure 1F). In contrast, expression of SCF and c-KIT was mainly restricted to epithelial cells in healthy colonic tissue (Figure 1, A and B). Taken together, these data highlight that colitis increases intestinal SCF$^{248}$ expression and immune cell recruitment (Figure 1, D and E).

### Targeted Deletion of SCF in IECs Does Not Influence Intestinal Homeostasis or Increase Susceptibility to DSS-induced Colitis

In addition to immune cells, epithelial cells have also been shown to produce SCF in mucosal tissues including the lungs and intestine.[15,26] Therefore, to explore the functional contribution of epithelial-expressed SCF during intestinal inflammation and repair, we generated mice with IEC-specific and tamoxifen-inducible deletion of SCF (*Kitlg*$^{ER\Delta IEC}$). These mice were generated by breeding *Kitlg* floxed mice (*Kitlg*$^{f/f}$) to mice constitutively expressing an ERT2-Cre fusion protein under control of *Villin* promoter.[35] The RT-qPCR analysis of colonic mucosal tissues revealed complete loss of SCF expression in IECs 30 days following tamoxifen injection in *Kitlg*$^{ER\Delta IEC}$ mice but not in control *Kitlg*$^{f/f}$ mice (**$P$ = .0043, Figure 2A). In contrast, similar SCF expression was detected in lamina propria cells for both *Kitlg*$^{ER\Delta IEC}$ and *Kitlg*$^{f/f}$ mice (Figure 2A). Histologic analysis of colonic mucosa in *Kitlg*$^{ER\Delta IEC}$ mice revealed normal architecture, with no gross abnormalities or

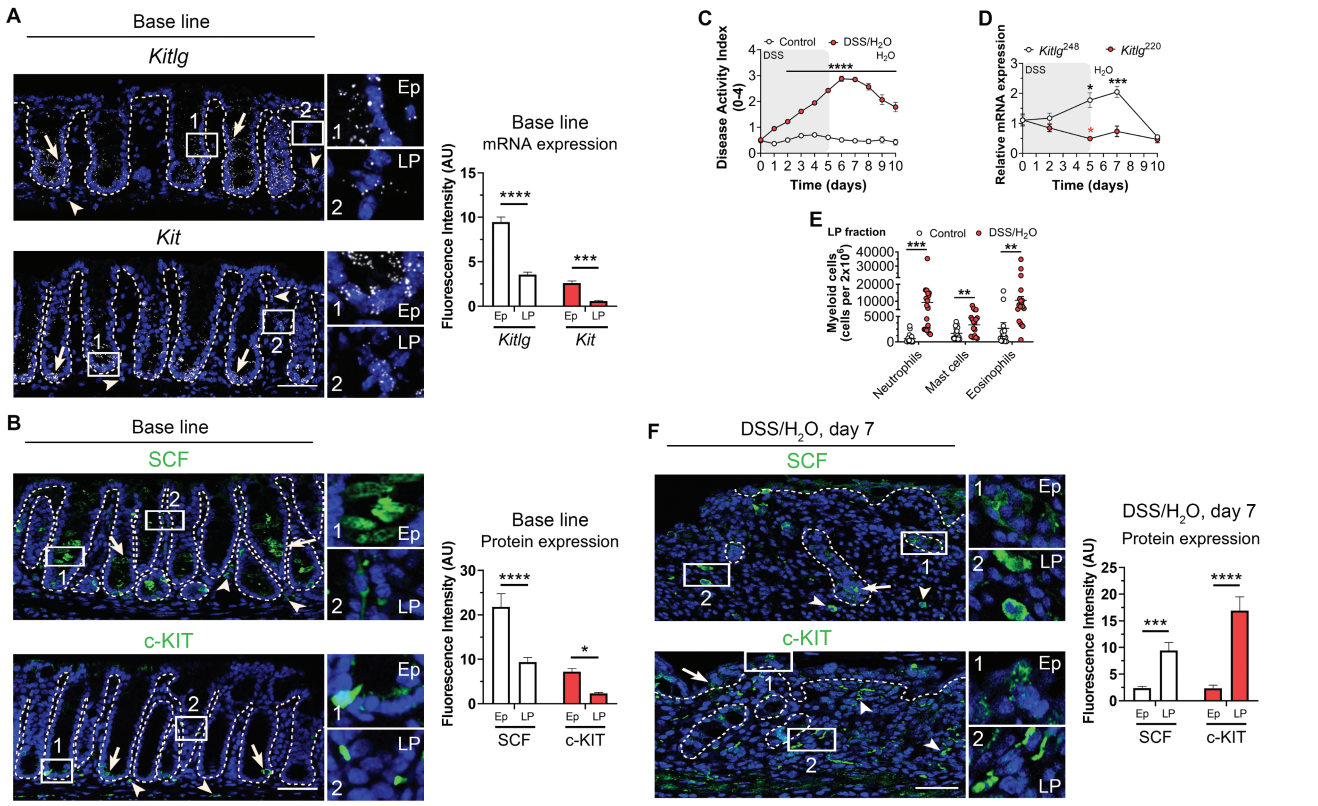


**Figure 1.** SCF$^{248}$ isoform expression is increased during acute colitis. A, Representative images of colonic tissue sections from WT C57BL/6J mice showing *Kitlg* (top) and *Kit* (bottom) mRNA expression (white) detected by RNAscope in situ hybridization. Expression in colonic epithelial cells (arrow and number 1 Ep inset) and lamina propria cells (arrowhead and number 2 lamina propria [LP] inset) are highlighted. Nuclei were stained with DAPI. Histograms show fluorescent intensity of *Kitlg* and *Kit* mRNA in epithelial cells and LP cells of the mouse colon. Data are combined from 2 independent experiments with a total of 3 fields per experiment and are expressed as means ± SEM. Significance was determined by 2-way ANOVA followed by Bonferroni's posttest. ***$P < .001$; ****$P < .0001$. Scale bar is 50 µm. Abbreviations: Ep, Epithelial; LP, lamina propria. B, Representative confocal microscopy images of SCF and c-KIT expression in colonic epithelial cells (arrow and number 1 Ep inset) and lamina propria cells (arrowhead and number 2 LP inset). Nuclei are stained with DAPI. Histograms show fluorescent intensity of SCF and c-KIT protein in epithelial cells and LP cells of the mouse colon. Data are combined from 2 independent experiments with a total of 3 fields per experiment and are expressed as means ± SEM. Significance was determined by 2-way ANOVA followed by Bonferroni's posttest. *$P < .05$; ****$P < .0001$. Scale bar is 50 µm. Abbreviations: Ep, Epithelial; LP, lamina propria. C, Disease activity index (DAI) score consisting of body weight, stool consistency, and presence of blood in feces in wild type C57BL/6J mice treated with 3% DSS for 5 days followed by 5 days of recovery on water (red circles). Disease activity index scores for control untreated mice are also shown (white circles). N = 11, Control; 15 DSS animals/group achieving 95% power where alpha value = 0.05 at day 10. Data are combined from 2 independent experiments and are expressed as means ± SEM. Significance was determined by 2-way ANOVA followed by Bonferroni's posttest. ****$P < .0001$. D, mRNA expression analysis for *Kitlg*$^{220}$ (red circles) and *Kitlg*$^{248}$ (white circles) was performed by qRT-PCR analyses of lamina propria cells isolated from the colons of control and DSS-treated mice. Results are mean ± SEM and are representative of 2 independent experiments, with at least 4 mice per condition. Significance was determined by 2-way ANOVA followed by Bonferroni's posttest. *$P <$ .05; ***$P < .001$. E, Flow cytometric analysis of lamina propria cells isolated from the colon of untreated mice (white circles) and DSS-treated mice (red circles) revealed increased colonic mucosal infiltration of neutrophils, mast cells, and eosinophils in DSS-treated animals at day 7. Each point denotes data from an individual mouse. N = 16 Control; 18 DSS animals/group achieving 95% power where alpha value = 0.05. Data are combined from 3 independent experiments and are expressed as means ± SEM. Statistical analysis was performed using multiple 2-tailed Student's *t* test. ***$P = .0003$ for Neutrophils; **$P = .0081$ for Mast cells; **$P = .0041$ for Eosinophils. F, Representative images of inflamed colonic tissue sections of DSS-treated mice showing SCF (top) and c-KIT (bottom) protein expression (green) detected by immunofluorescence. Expression in colonic epithelial cells (arrow and number 1 Ep inset) and lamina propria cells (arrowhead and number 2 LP inset) are highlighted. Nuclei were stained with DAPI. Histograms show fluorescence intensity of SCF and c-KIT protein expression in epithelial cells and LP cells of the mouse colon. Data are combined from 2 independent experiments with a total of 3 fields per experiment and are expressed as means ± SEM. Significance was determined by 2-way ANOVA followed by Bonferroni's posttest. ***$P < .001$; ****$P < .0001$. Scale bar is 50 µm. Abbreviations: Ep, Epithelial; LP, lamina propria.

signs of mucosal inflammation (Figure 2B). These results suggest that specific loss of SCF in IECs does not affect baseline intestinal mucosal homeostasis.

We next examined the role of epithelial expressed SCF during intestinal injury and repair. Surprisingly, data revealed no significant difference in disease severity during either the inflammatory or recovery phases when *Kitlg*$^{ER\Delta IEC}$ or control *Kitlg*$^{f/f}$ mice were subjected to DSS-induced colitis followed by recovery (Figure 2C). Subsequent experiments were performed to determine the effects of intestinal epithelial–specific loss of SCF in a model of chronic intestinal inflammation that employs multiple cycles of DSS administration followed by a recovery period. As expected, *Kitlg*$^{ER\Delta IEC}$ and control *Kitlg*$^{f/f}$ mice developed escalating clinical colitis when subjected to repeated alternating cycles of DSS administration and water recovery. However, no significant difference in disease severity was observed for *Kitlg*$^{ER\Delta IEC}$ compared with control *Kitlg*$^{f/f}$ littermates (Figure 2D). These findings indicate that loss of SCF in IECs does not impact disease severity in response to acute or chronic DSS-induced intestinal inflammation. Finally,

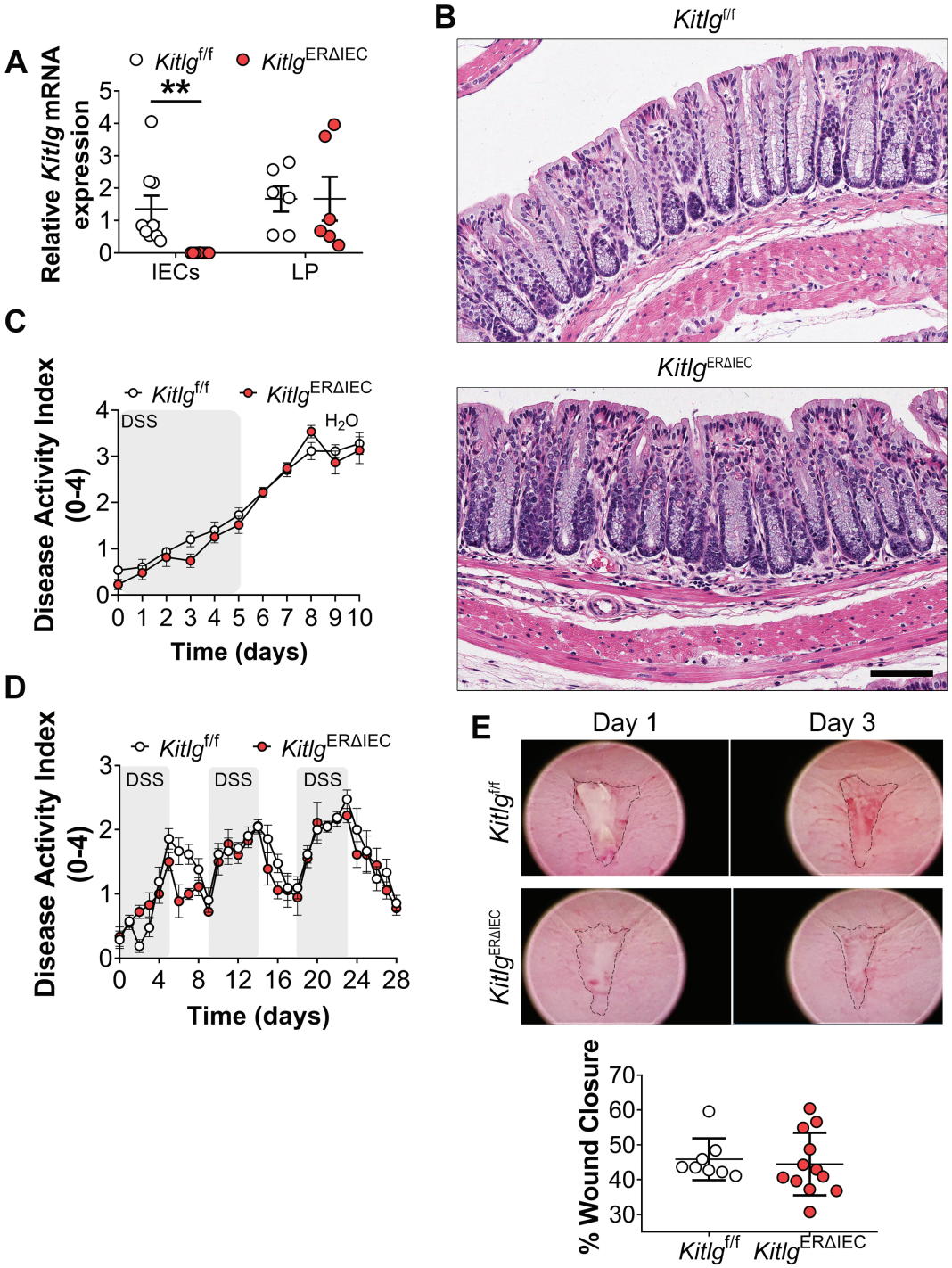


**Figure 2.** Loss of SCF expression in intestinal epithelial cells (IECs) does not alter intestinal mucosal architecture or susceptibility to DSS-induced colitis. A, RT-qPCR analyses of SCF expression in the colon of *Kitlg*$^{ERΔIEC}$ mice and control littermate *Kitlg*$^{f/f}$ mice 30 days following injection with tamoxifen. Shown is *Kitlg* (SCF) mRNA expression in colonic IECs and lamina propria (LP) cells isolated from *Kitlg*$^{ERΔIEC}$ or control *Kitlg*$^{f/f}$ mice. Data points represent mRNA expression values from individual mice, which were normalized to the housekeeping gene ribosomal protein 18 (Rps18). Each point denotes data from individual mice. For IECs, N = 9 *Kitlg*$^{f/f}$; 9 *Kitlg*$^{ERΔIEC}$ animals/group achieving 95% power where alpha value = 0.05. For LP cells, 6 *Kitlg*$^{f/f}$; 6 *Kitlg*$^{ERΔIEC}$ animals/group. Graph represents values obtained from 3 independent experiments with a minimum of 6 mice per group. Data are expressed as means ± SEM. Significance is determined by a 2-tailed Student's *t* test with Welch's correction. $^{**}P = .0043$. B, Representative images of H&E staining of sections of colonic Swiss roll mounts showing a gross mucosal architecture of *Kitlg*$^{ERΔIEC}$ vs *Kitlg*$^{f/f}$ mice. Scale bar is 90 μm. C-D, Loss of SCF expression in IECs does not exacerbate acute or chronic colitis as reflected by similar DAI scoring for *Kitlg*$^{f/f}$ and *Kitlg*$^{ERΔIEC}$ mice. Data were generated from one experiment with at least 6 to 7 mice per group and are expressed as means ± SEM. Significance was determined by 2-way ANOVA followed by Bonferroni's posttest. E, Analysis of wound closure at day 3 postbiopsy wounding revealed no differences in wound repair in the absence of IEC-expressed SCF. Dots represent the mean value from 3 to 5 wounds from individual mice. Data are combined values of 2 independent experiments with a total of 8 to 12 mice for *Kitlg*$^{f/f}$ and *Kitlg*$^{ERΔIEC}$ groups and are expressed as mean ± SEM.

the contribution of IEC-produced SCF to intestinal mucosal wound healing was investigated using a third model of injury and repair that employs a miniaturized endoscopic to create biopsy-induced wounds in the distal colon. In line with our previous observations, *Kitlg*$^{ER\Delta IEC}$ and control *Kitlg*$^{f/f}$ mice exhibited similar rates of wound healing 3 days after biopsy-induced injury (Figure 2E). When combined, these results highlight the importance of nonepithelial cell–produced SCF during colitis and mucosal repair in the gut.

### Neutralization of SCF$^{248}$ and SCF$^{220}$ Isoforms Promote Colonic Repair

To better assess the functional role of SCF during intestinal inflammation and repair, we utilized an inhibitory anti-SCF polyclonal antibody (SCF$^{248\&220}$) developed in the Lukacs laboratory and validated as previously reported[26]; 3 mg/mouse anti-SCF$^{248\&220}$ or rabbit anti-IgG control antibodies (Abs) were administered on days 5 and 7 by intraperitoneal injection before assessment of DAI during DSS-induced colitis and recovery. Data revealed significantly decreased inflammation, as reflected by reduced stool index (SI) and DAI scores on days 7 and 8 in mice injected with anti-SCF$^{248\&220}$ antibody (**$P$ < .01, ***$P$ < .001, Figure 3, A and B). Histological analysis of colonic tissue from IgG-treated control mice showed severe mucosal inflammation characterized by superficial ulceration, crypt destruction, mucosal damage, and leukocyte infiltration. In contrast, analysis of colonic mucosa from mice injected with neutralizing anti-SCF$^{248\&220}$ Ab revealed significantly reduced levels of mucosal inflammation and epithelial loss/erosion, and ulceration, that was reflected by a 70% reduction in the Histological Colitis Score (HCS, ***$P$ = .0006, Figure 3, C and D). Compared with mice injected with control Ab, flow cytometry analysis of infiltrating leukocyte populations in the lamina propria of DSS-treated mice revealed significantly decreased recruitment of neutrophils upon anti-SCF$^{248\&220}$ Ab administration. In addition, mast cells and eosinophil populations also displayed a downward trend. (*$P$ = .04, Supplemental figures 1 and 2). In addition to immune cell infiltration, intestinal inflammation is also characterized by increased pro-inflammatory cytokine expression. Therefore, we investigated effects of SCF neutralization on expression of pro-inflammatory cytokines in the lamina propria during DSS-induced colitis. Data revealed significantly decreased expression of the proinflammatory cytokines *Tnfa*, *Il17a*, and *S100a9*, following SCF neutralization in DSS-treated mice (*Tnfa*, *$P$ = .0481; *Il17a*, *$P$ = .0355; *S100a9*, **$P$ = .0018, Supplemental Figure 3). Taken together, our findings suggest that the blockade of SCF induces an anti-inflammatory response during DSS induced colitis.

We next determined effects of SCF inhibition during mucosal repair following biopsy-induced colonic injury. For these assays, anti-SCF$^{248\&220}$ or IgG control Abs were injected directly into colonic wounds before assessment of wound closure 1 and 3 days postinjury. Importantly, a significantly increased wound repair was observed at day 3 in mice injected with anti-SCF$^{248\&220}$ Ab compared with IgG control Ab injected animals (***$P$ = .0002, Figure 3E). Taken together, data demonstrate that SCF inhibition enhances repair following DSS-induced colitis and improves rates of mucosal repair following mechanical injury in the colon by reducing myeloid cell infiltration into the lamina propria.

Given the robust upregulation of SCF$^{248}$ observed during intestinal inflammation (Figure 1D), we next determined effects of inhibition of specific isoforms of SCF on intestinal repair using a monoclonal antibody (mAb) that specifically inhibits the cleavable SCF$^{248}$ isoform.[27] As was observed for total SCF neutralization, administration of an inhibitory anti-SCF$^{248}$ antibody significantly improved recovery from DSS-induced colitis as determined by a significant reduction in SI and DAI on days 7 and 8 relative to IgG control Ab injected mice (*$P$ < .05, **$P$ < .01, ***$P$ < .001, Figure 4, A and B). Histological evaluation of colonic mucosa revealed significantly reduced mucosal inflammation and ulceration in mice treated with anti-SCF$^{248}$ mAb vs IgG control Ab (**$P$ = .0088, Figure 4, C and D). Taken together, these findings suggest that specific neutralization of SCF$^{248}$ drives mucosal repair in the colon.

## Discussion

The importance of SCF/c-KIT signaling in driving stem cell survival, proliferation, and differentiation during hematopoiesis, gametogenesis, and melanogenesis has been well documented.[36] Furthermore, although increased SCF expression has been reported in the inflamed mucosa of individuals with IBD,[15,16] the role of SCF/c-KIT signaling during intestinal inflammation and repair has not been explored. Here we report differential expression of SCF and c-KIT in IECs along the crypt luminal axis of the colon. Data showing SCF expression in colonic goblet cells are in line with previous reports demonstrating a functional interplay between SCF/c-KIT and mucin-2 production/mucus secretion by goblet cells in colorectal adenocarcinoma.[37,38] Our data also revealed SCF and c-KIT expression in stem cells at the crypt base, which is consistent with previously published cell-specific expression patterns identified by multicolor fluorescence-activated cell sorting and multiplexed single-cell qRT-PCR.[39] Specifically, this previous study identified that SCF expression was detected predominantly in Lgr5+ stem cell populations; but it is important to note that c-KIT expression was found in small intestine Paneth cells and a subset of colonic goblet cells, classified as Paneth-like cells in the crypt-base. Taken together, these data suggest that at least 2 different crypt epithelial cell populations produce SCF and c-KIT during homeostatic conditions in the murine colon. Further studies will be required to determine if SCF produced by goblet cells vs Lgr5+ cells mediates differential downstream signaling and functional outcomes during intestinal inflammation and repair.

Data shown here identifying IECs to be a source of SCF and c-KIT during mucosal homeostasis are supported by previous work reporting increased expression of both molecules in IECs relative to lamina propria cells.[15] Stem cell factor and c-KIT expression have been previously reported in lamina propria cells, including enteric nervous cells, mast cells, and Cajal interstitial cells.[40–44] However, further studies are needed to determine which specific lamina propria cells (structural or immune) express SCF and c-KIT in order to regulate mucosal repair.

The clinical relevance of SCF expression to human intestinal disease is highlighted by a previous study demonstrating increased SCF expression in the epithelial lining, mucosa, and submucosa from individuals with UC and CD.[15] Similarly, exposure to cholera toxin (CT) or *Salmonella typhimurium* has been shown to induce expression of SCF in the intestinal

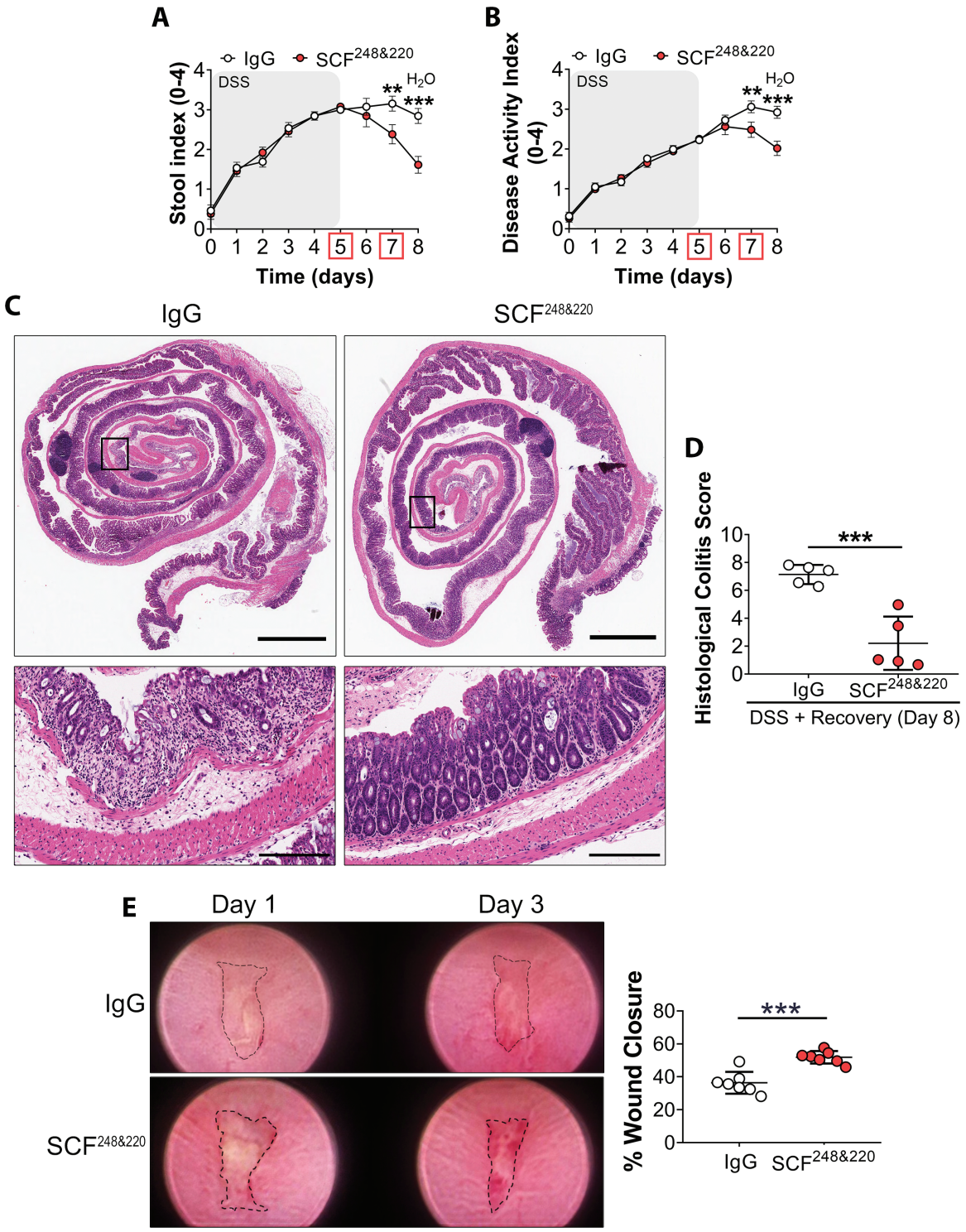


**Figure 3.** Neutralization of SCF enhances mucosal wound repair in the colon. A-B, SI and DAI scores from mice injected with 3 mg/mouse anti-SCF$^{248\&220}$ Ab or IgG control Ab at days 5 and 7 during DSS-induced colitis and repair. N = 13 DSS + IgG Ab; 13 DSS + SCF$^{248\&220}$ Ab animals/group achieving 95% power where alpha value = 0.05 at day 8. Data are combined from 2 independent experiments and are expressed as means ± SEM. Significance is determined by 2-way ANOVA followed by Bonferroni's posttest. $^{**}P < .01$; $^{***}P < .001$. C, Representative images of H&E staining of sections of Swiss roll mounts from the distal colon of mice treated with either anti-SCF$^{248\&220}$ or IgG antibodies. Colonic tissues were harvested on day 8 of the experiment. Scale bars are 2 mm (whole colon) and 200 µm (inset). D, Calculation of histological colitis score of injury/ulceration that represents the ratio of the length of injured/ulcerated areas (≥50% crypt loss) relative to the entire colon length reveals less mucosal ulcerations in anti-SCF$^{248\&220}$ Ab-treated mice compared with controls. Dots represent individual mice. N = 5 DSS + IgG Ab; 5 DSS + SCF$^{248\&220}$ Ab animals/group achieving 95% power where alpha value = 0.05 at day 8. Data are combined from 2 independent experiments and are expressed as means ± SEM. Significance is determined by a 2-tailed Student's *t* test. $^{***}P = .0006$. E, Neutralization of SCF improves mucosal wound healing following biopsy-induced injury; 10 µg of SCF$^{248\&220}$ or IgG antibodies were injected into the wound bed on day 1. Analysis of wound closure at day 3 postbiopsy wounding revealed a significant increase in wound repair following SCF neutralization. Dots represent the mean value calculated from the analysis of 3 to 5 wounds from individual mice. N = 7 DSS + IgG Ab; 7 DSS + SCF$^{248\&220}$ Ab animals/group achieving 95% power where alpha value = 0.05 at day 3. Data are combined from 2 independent experiments and are expressed as means ± SEM. Significance is determined by a 2-tailed Student's *t* test. $^{***}P = .0002$.

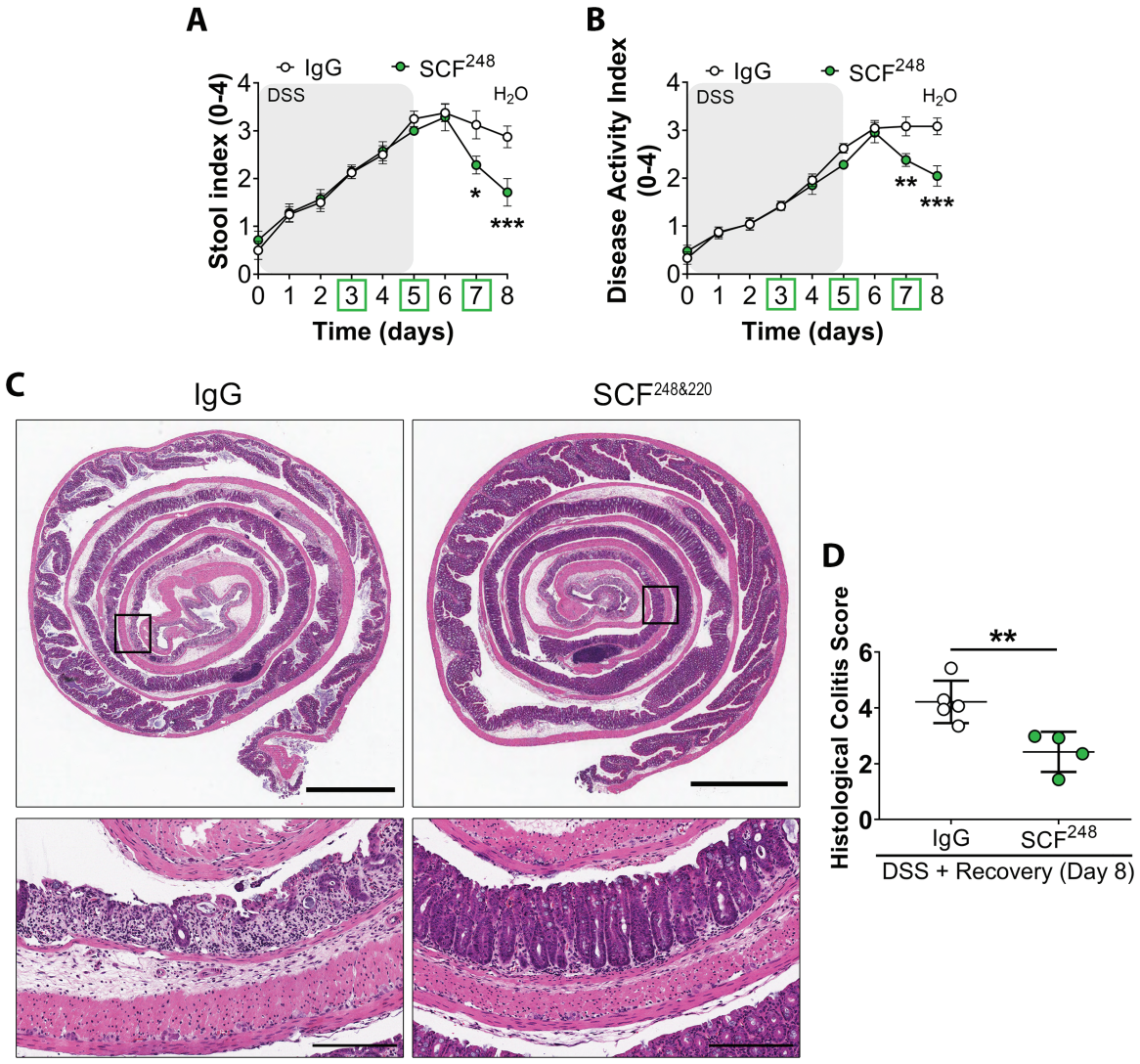


**Figure 4.** Specific neutralization of the SCF$^{248}$ isoform promotes mucosal recovery after DSS-induced injury. Wild-type C57BL/6J mice were subjected to DSS-induced colitis followed by water recovery with 0.4 mg/mouse of anti-SCF$^{248}$ Ab or IgG control Ab administrated by i.p. injection at days 3, 5, and 7. (A, B) Anti-SCF$^{248}$ Ab treatment enhanced recovery from DSS-induced colitis as reflected by significantly decreased SI and DAI scoring compared with IgG control Ab-treated mice. N = 8 DSS + IgG Ab; 7 DSS + SCF$^{248}$ Ab animals/group achieving 95% power where alpha value = 0.05 at day 8. Data are combined from 2 independent experiments and are expressed as means ± SEM. Significance is determined by 2-way ANOVA followed by Bonferroni's posttest. *$p < .05$, **$p < .01$; ***$p < .001$. C, Representative H&E images of sections of Swiss roll mounts from the distal colon of DSS-treated mice injected intraperitoneally with either anti-SCF$^{248}$ or IgG antibodies. Colonic tissues were harvested at day 8 of the experiment. Scale bars are 2 mm (whole colon) and 200 µm (inset). D, Histological colitis score showing reduced mucosal ulceration in anti-SCF$^{248}$ Ab-treated mice compared with controls. Dots represent individual mice. N = 5 DSS + IgG Ab; 4 DSS + SCF$^{248}$ Ab animals/group achieving 95% power where alpha value = 0.05 on day 8. Data represent one experiment and are expressed as mean ± SEM. Significance is determined by a 2-tailed Student's *t* test on day 8. **$P = .0088$.

tract in vivo and the murine intestinal epithelial cell line MODE-K.[17,18] Given the complex mechanisms that govern SCF signaling, an increased understanding of the role of specific SCF isoforms is of paramount importance. For example, previous work has shown that soluble and membrane-bound SCF isoforms activate different signaling pathways downstream of c-KIT in order to affect distinct biologic outcomes.[45,46] Here we show for the first time that the cleavable form of SCF (SCF$^{248}$) can be specifically inhibited to promote intestinal repair and block colitis in mice subjected to either mechanical biopsy or DSS treatment, respectively. In contrast to our findings, a recent study that did not consider the effects of specific SCF isoforms suggested that SCF signaling promotes epithelial tissue-regenerative responses mediated by Paneth cell de-differentiation in vitro.[15] It is likely that differing effects observed on repair can also be attributed to the fact that this study was performed in vitro in the absence of nonepithelial cell populations.

The importance of SCF$^{248}$ to mucosal inflammation is supported by previous reports demonstrating increased SCF$^{248}$ isoform expression and involvement in inflammatory conditions such as pulmonary fibrosis and chronic allergic asthma.[27,47] Consistent with SCF$^{248}$ playing an important role in intestinal pathobiology, increased levels of soluble SCF have been reported in the plasma of individuals with UC and CD.[30] Importantly, elevated SCF$^{248}$ expression levels during DSS-induced colitis coincided with increased infiltration of neutrophils, mast cells, and eosinophils. Given that previous studies have demonstrated that mast cells[42] and eosinophils[48] produce SCF during inflammation, it is likely that these cells are a source of SCF$^{248}$

in inflamed intestinal tissues. Similar findings in terms of mast cell–produced SCF[248] have previously been reported in inflamed lung tissues.[12,26,49,50] However, future studies are required to determine if other cells such as neutrophils, enteric nervous cells, or fibroblasts[51,52] produce SCF[248] during intestinal inflammation. Importantly, both mast cells and eosinophils utilize SCF for activation and survival and may be part of the pathogenesis associated with disease severity.

To better understand contributions of SCF produced by individual mucosal cell types during colitis, we generated mice with intestinal epithelial-specific deletion of SCF (*Kitlg*$^{ER\Delta IEC}$). Surprisingly, loss of expression of epithelial SCF did not influence susceptibility to or recovery from DSS-induced colitis, suggesting that SCF produced by nonepithelial cell populations is important for IBD pathogenesis. Therapeutic benefits of targeting SCF[248] have been demonstrated for inflammatory conditions, including chronic asthma, pulmonary fibrosis, and food allergen-induced intestinal disease. Importantly, these studies demonstrated that antibody-mediated inhibition of SCF[248] decreased lung pathogenesis and resulted in decreased pro-inflammatory cytokine production and reduced levels of c-KIT+ innate immune cells, including mast cells, eosinophils, and ILC2s.[27,47,53] In support of this, it has been previously reported that SCF[248] neutralization reduced infiltration of mast cells and eosinophils into the small intestine in response to food allergy[53] and reduced immune cell influx during chronic asthmatic disease in vivo.[47] Furthermore, intrapulmonary instillation of SCF antisense oligonucleotides during allergen challenges was shown to reduce the infiltration of eosinophils into the lung.[49]

Here we report that SCF inhibition decreased neutrophil infiltration into inflamed colonic mucosal tissues. This decrease in neutrophil trafficking may be secondary to decreased eosinophil numbers and/or activation observed upon SCF inhibition, as eosinophils are known to play an important role in trafficking and activation of neutrophils to sites of intestinal inflammation through release of chemotactic factors including IL-8, CXCL5, and GM-CSF.[54–57] Although the acute DSS plus recover injury model employed in this study recapitulates many events important for the initiation and persistence of inflammation in human IBD, this model can be considered most relevant for studying a UC-like intestinal inflammation.[58] Furthermore, the acute DSS model is particularly useful for studying the contributions of innate immune cells to intestinal inflammation independent from adaptative immune response considerations.[59] Given these limitations, future studies will explore effects of SCF[248] blockade in other well-established mouse CD-like models, such as acute and chronic 2,4,6-trinitrobenzene sulfonic acid (TNBS)/ethanol exposure[59–61] and the spontaneous CD-like colitis model using SAMP1/Yit mice,[62] which involve an adaptive immune response. In conclusion, our studies highlight that specific inhibition of SCF[248] during intestinal inflammation promotes mucosal healing, suggesting that anti-SCF neutralizing antibodies have potential as therapeutic agents to drive intestinal repair and reduce the severity of symptoms for individuals with IBD.

## Supplementary Data

Supplementary data is available at *Inflammatory Bowel Diseases* online.

## Acknowledgments

The authors thank Dr. Roland Hilgarth for technical assistance in the generation of *Kitlg*$^{f/f}$ and *Kitlg*$^{ER\Delta IEC}$ mice. We thank the Transgenic and Gene Targeting Core, Microscopy and Image Analysis Laboratory, and the Unit for Laboratory Animal Medicine (ULAM) at the University of Michigan Medical School.

## Author Contributions

V.G.-H. designed and performed experiments, analyzed and interpreted data, as well as drafted and edited the manuscript. A.R.-S., J.M., and J.B. analyzed and interpreted data, drafted and edited the manuscript. V.A., M.K., S.F., D.B., and M.Q. designed and performed experiments, analyzed and interpreted data. C.A.P. helped with the design of experiments and manuscript editing. A.N. supervised the study, designed experiments, provided resources, and helped with manuscript organization and editing.

## Funding

This work was supported by the following grants: Crohn's and Colitis Foundation Research Fellowships 623536 (A.R.-S.), and 934934 (J.M.), National Institutes of Health R01 DK055679 (A.N.), and University of Michigan Center for Gastrointestinal Research (UMCGR), (NIDDK 5P30DK034933).

## Conflicts of Interest

All authors declare that they have no conflicts of interest.

## References

1 Podolsky DK. Inflammatory bowel disease. *N Engl J Med*. 2002;347(6):417-429.
2 Bouma G, Strober W. The immunological and genetic basis of inflammatory bowel disease. *Nat Rev Immunol*. 2003;3(7):521-533.
3 Dahlhamer JM, Zammitti EP, Ward BW, Wheaton AG, Croft JB. Prevalence of Inflammatory Bowel Disease Among Adults Aged >/=18 Years - United States, 2015. *MMWR Morb Mortal Wkly Rep*. 2016;65(42):1166-1169.
4 Collaborators GBDIBD. The global, regional, and national burden of inflammatory bowel disease in 195 countries and territories, 1990-2017: a systematic analysis for the Global Burden of Disease Study 2017. *Lancet Gastroenterol Hepatol*. 2020;5(1):17-30.
5 Li K, Feng C, Chen H, Feng Y, Li J. Trends in worldwide research in inflammatory bowel disease over the period 2012-2021: a bibliometric study. *Front Med (Lausanne)*. 2022;9:880553.
6 de Souza HS, Fiocchi C. Immunopathogenesis of IBD: current state of the art. *Nat Rev Gastroenterol Hepatol*. 2016;13(1):13-27.
7 Ungaro R, Mehandru S, Allen PB, Peyrin-Biroulet L, Colombel JF. Ulcerative colitis. *Lancet*. 2017;389(10080):1756-1770.
8 Gisbert JP, Chaparro M. Predictors of primary response to biologic treatment [anti-TNF, vedolizumab, and ustekinumab] in patients with inflammatory bowel disease: from basic science to clinical practice. *J Crohns Colitis*. 2020;14(5):694-709.
9 Williams DE, Eisenman J, Baird A, et al. Identification of a ligand for the c-kit proto-oncogene. *Cell*. 1990;63(1):167-174.
10 Flanagan JG, Leder P. The kit ligand: a cell surface molecule altered in steel mutant fibroblasts. *Cell*. 1990;63(1):185-194.
11 Zsebo KM, Williams DA, Geissler EN, et al. Stem cell factor is encoded at the Sl locus of the mouse and is the ligand for the c-kit tyrosine kinase receptor. *Cell*. 1990;63(1):213-224.

12 Lukacs NW, Kunkel SL, Strieter RM, et al. The role of stem cell factor (c-kit ligand) and inflammatory cytokines in pulmonary mast cell activation. *Blood*. 1996;87(6):2262-2268.
13 Carter EL, O'Herrin S, Woolery C, Jack Longley B. Epidermal stem cell factor augments the inflammatory response in irritant and allergic contact dermatitis. *J Invest Dermatol*. 2008;128(7):1861-1863.
14 Longley BJ, Jr, Morganroth GS, Tyrrell L, et al. Altered metabolism of mast-cell growth factor (c-kit ligand) in cutaneous mastocytosis. *N Engl J Med*. 1993;328(18):1302-1307.
15 Schmitt M, Schewe M, Sacchetti A, et al. Paneth cells respond to inflammation and contribute to tissue regeneration by acquiring stem-like features through SCF/c-Kit signaling. *Cell Rep*. 2018;24(9):2312-2328 e2317.
16 Comar M, Secchiero P, De Lorenzo E, Martelossi S, Tommasini A, Zauli G. JCV+ patients with inflammatory bowel disease show elevated plasma levels of MIG and SCF. *Inflamm Bowel Dis*. 2012;18(6):1194-1196.
17 Klimpel GR, Chopra AK, Langley KE, et al. A role for stem cell factor and c-kit in the murine intestinal tract secretory response to cholera toxin. *J Exp Med*. 1995;182(6):1931-1942.
18 Klimpel GR, Langley KE, Wypych J, Abrams JS, Chopra AK, Niesel DW. A role for stem cell factor (SCF): c-kit interaction(s) in the intestinal tract response to *Salmonella typhimurium* infection. *J Exp Med*. 1996;184(1):271-276.
19 Fischer OM, Streit S, Hart S, Ullrich A. Beyond herceptin and gleevec. *Curr Opin Chem Biol*. 2003;7(4):490-495.
20 Fiedler W, Mesters R, Tinnefeld H, et al. A phase 2 clinical study of SU5416 in patients with refractory acute myeloid leukemia. *Blood*. 2003;102(8):2763-2767.
21 Margulies D, Opatowsky Y, Fletcher S, et al. Surface binding inhibitors of the SCF-KIT protein-protein interaction. *ChemBioChem*. 2009;10(12):1955-1958.
22 Garcia-Hernandez V, Neumann PA, Koch S, Lyons R, Nusrat A, Parkos CA. Systematic scoring analysis for intestinal inflammation in a murine dextran sodium sulfate-induced colitis model. *J Vis Exp*. 2021;(168):e62135.
23 Reed M, Luissint AC, Azcutia V, et al. Epithelial CD47 is critical for mucosal repair in the murine intestine in vivo. *Nat Commun*. 2019;10(1):5004.
24 Flemming S, Luissint AC, Kusters DHM, et al. Desmocollin-2 promotes intestinal mucosal repair by controlling integrin-dependent cell adhesion and migration. *Mol Biol Cell*. 2020;31(6):407-418.
25 Quiros M, Nishio H, Neumann PA, et al. Macrophage-derived IL-10 mediates mucosal repair by epithelial WISP-1 signaling. *J Clin Invest*. 2017;127(9):3510-3520.
26 Lukacs NW, Strieter RM, Lincoln PM, et al. Stem cell factor (c-kit ligand) influences eosinophil recruitment and histamine levels in allergic airway inflammation. *J Immunol*. 1996;156(10):3945-3951.
27 Rasky A, Habiel DM, Morris S, et al. Inhibition of the stem cell factor 248 isoform attenuates the development of pulmonary remodeling disease. *Am J Physiol Lung Cell Mol Physiol*. 2020;318(1):L200-l211.
28 Leoni G, Neumann PA, Kamaly N, et al. Annexin A1-containing extracellular vesicles and polymeric nanoparticles promote epithelial wound repair. *J Clin Invest*. 2015;125(3):1215-1227.
29 Wang F, Flanagan J, Su N, et al. RNAscope: a novel in situ RNA analysis platform for formalin-fixed, paraffin-embedded tissues. *J Mol Diagn*. 2012;14(1):22-29.
30 Andersson E, Bergemalm D, Kruse R, et al. Subphenotypes of inflammatory bowel disease are characterized by specific serum protein profiles. *PLoS One*. 2017;12(10):e0186142e0186142.
31 Al-Muhsen SZ, Shablovsky G, Olivenstein R, Mazer B, Hamid Q. The expression of stem cell factor and c-kit receptor in human asthmatic airways. *Clin Exp Allergy*. 2004;34(6):911-916.
32 Smith KA, Zsebo KM. Measurement of human and murine stem cell factor (c-kit ligand). *Curr Protoc Immunol*. 2001;Chapter 6:Unit 6 17.
33 Da Silva CA, Reber L, Frossard N. Stem cell factor expression, mast cells and inflammation in asthma. *Fundam Clin Pharmacol*. 2006;20(1):21-39.
34 Arseneau KO, Cominelli F. Targeting leukocyte trafficking for the treatment of inflammatory bowel disease. *Clin Pharmacol Ther*. 2015;97(1):22-28.
35 el Marjou F, Janssen KP, Chang BH, et al. Tissue-specific and inducible Cre-mediated recombination in the gut epithelium. *Genesis*. 2004;39(3):186-193.
36 Lennartsson J, Ronnstrand L. Stem cell factor receptor/c-Kit: from basic science to clinical implications. *Physiol Rev*. 2012;92(4):1619-1649.
37 Li G, Yang S, Shen P, et al. SCF/c-KIT signaling promotes mucus secretion of colonic goblet cells and development of mucinous colorectal adenocarcinoma. *Am J Cancer Res*. 2018;8(6):1064-1073.
38 Shen P, Yang S, Sun H, et al. SCF/c-KIT Signaling Increased Mucin2 Production by Maintaining Atoh1 Expression in Mucinous Colorectal Adenocarcinoma. *Int J Mol Sci* . 2018;19(5):1541-1553.
39 Rothenberg ME, Nusse Y, Kalisky T, et al. Identification of a cKit(+) colonic crypt base secretory cell that supports Lgr5(+) stem cells in mice. *Gastroenterology*. 2012;142(5):1195-1205.e6.
40 Al-Sajee D, Huizinga JD. interstitial cells of cajal: pathology, injury and repair. *Sultan Qaboos Univ Med J*. 2012;12(4):411-421.
41 Maeda H, Yamagata A, Nishikawa S, et al. Requirement of c-kit for development of intestinal pacemaker system. *Development*. 1992;116(2):369-375.
42 Welker P, Grabbe J, Gibbs B, Zuberbier T, Henz BM. Human mast cells produce and differentially express both soluble and membrane-bound stem cell factor. *Scand J Immunol*. 1999;49(5):495-500.
43 Nocka K, Majumder S, Chabot B, et al. Expression of c-kit gene products in known cellular targets of W mutations in normal and W mutant mice--evidence for an impaired c-kit kinase in mutant mice. *Genes Dev*. 1989;3(6):816-826.
44 Finotto S, Mekori YA, Metcalfe DD. Glucocorticoids decrease tissue mast cell number by reducing the production of the c-kit ligand, stem cell factor, by resident cells: in vitro and in vivo evidence in murine systems. *J Clin Invest*. 1997;99(7):1721-1728.
45 Trieselmann NZ, Soboloff J, Berger SA. Mast cells stimulated by membrane-bound, but not soluble, steel factor are dependent on phospholipase C activation. *Cell Mol Life Sci*. 2003;60(4):759-766.
46 Chuyen A, Rulquin C, Daian F, et al. The Scf/Kit pathway implements self-organized epithelial patterning. *Dev Cell*. 2021;56(6):795-810.e7.
47 Fonseca W, Rasky AJ, Ptaschinski C, et al. Group 2 innate lymphoid cells (ILC2) are regulated by stem cell factor during chronic asthmatic disease. *Mucosal Immunol*. 2019;12(2):445-456.
48 Hartman M, Piliponsky AM, Temkin V, Levi-Schaffer F. Human peripheral blood eosinophils express stem cell factor. *Blood*. 2001;97(4):1086-1091.
49 Finotto S, Buerke M, Lingnau K, Schmitt E, Galle PR, Neurath MF. Local administration of antisense phosphorothioate oligonucleotides to the c-kit ligand, stem cell factor, suppresses airway inflammation and IL-4 production in a murine model of asthma. *J Allergy Clin Immunol*. 2001;107(2):279-286.
50 Berlin AA, Lincoln P, Tomkinson A, Lukacs NW. Inhibition of stem cell factor reduces pulmonary cytokine levels during allergic airway responses. *Clin Exp Immunol*. 2004;136(1):15-20.
51 Heinrich MC, Dooley DC, Freed AC, et al. Constitutive expression of steel factor gene by human stromal cells. *Blood*. 1993;82(3):771-783.
52 Linenberger ML, Jacobson FW, Bennett LG, Broudy VC, Martin FH, Abkowitz JL. Stem cell factor production by human marrow stromal fibroblasts. *Exp Hematol*. 1995;23(10):1104-1114.
53 Ptaschinski C, Rasky AJ, Fonseca W, Lukacs NW. Stem cell factor neutralization protects from severe anaphylaxis in a murine model of food allergy. *Front Immunol*. 2021;12:604192.
54 Braun RK, Franchini M, Erard F, et al. Human peripheral blood eosinophils produce and release interleukin-8 on stimulation with calcium ionophore. *Eur J Immunol*. 1993;23(4):956-960.

55 Baggiolini M, Walz A, Kunkel SL. Neutrophil-activating peptide-1/interleukin 8, a novel cytokine that activates neutrophils. *J Clin Invest*. 1989;84(4):1045-1049.
56 Persson T, Monsef N, Andersson P, et al. Expression of the neutrophil-activating CXC chemokine ENA-78/CXCL5 by human eosinophils. *Clin Exp Allergy.* 2003;33(4):531-537.
57 Khajah M, Millen B, Cara DC, Waterhouse C, McCafferty DM. Granulocyte-macrophage colony-stimulating factor (GM-CSF): a chemoattractive agent for murine leukocytes in vivo. *J Leukoc Biol*. 2011;89(6):945-953.
58 Boismenu R, Chen Y. Insights from mouse models of colitis. *J Leukoc Biol*. 2000;67(3):267-278.
59 Dieleman LA, Ridwan BU, Tennyson GS, Beagley KW, Bucy RP, Elson CO. Dextran sulfate sodium-induced colitis occurs in severe combined immunodeficient mice. *Gastroenterology.* 1994;107(6):1643-1652.
60 Morris GP, Beck PL, Herridge MS, Depew WT, Szewczuk MR, Wallace JL. Hapten-induced model of chronic inflammation and ulceration in the rat colon. *Gastroenterology.* 1989;96(3):795-803.
61 Neurath MF, Fuss I, Kelsall BL, Stuber E, Strober W. Antibodies to interleukin 12 abrogate established experimental colitis in mice. *J Exp Med*. 1995;182(5):1281-1290.
62 Matsumoto S, Okabe Y, Setoyama H, et al. Inflammatory bowel disease-like enteritis and caecitis in a senescence accelerated mouse P1/Yit strain. *Gut*. 1998;43(1):71-78.